

Melanopsin and rod–cone photoreceptive systems account for all major accessory visual functions in mice

S. Hattar*, R. J. Lucas†, N. Mrosovsky‡, S. Thompson†, R. H. Douglas§, M. W. Hankins†, J. Lem||, M. Biel¶, F. Hofmann#, R. G. Foster† & K.-W. Yau*

* Howard Hughes Medical Institute and Department of Neuroscience, Johns Hopkins University School of Medicine, Baltimore, Maryland 21205, USA

† Department of Integrative and Molecular Neuroscience, Division of Neuroscience and Psychological Medicine, Faculty of Medicine, Imperial College London, Charing Cross Campus, London W6 8RF, UK

‡ Departments of Zoology, Physiology and Psychology, University of Toronto, Toronto, Ontario M5S 3G5, Canada

§ Applied Vision Research Centre, Department of Optometry and Visual Science, City University, Northampton Square, London EC1V 0HB, UK

|| Department of Ophthalmology, Tufts University School of Medicine, Boston, Massachusetts 02111, USA

¶ Lehrstuhl Pharmakologie für Naturwissenschaften, Zentrum für Pharmaforschung, Ludwig-Maximilians Universität München, 81377 München, Germany

Institut für Pharmakologie und Toxikologie, Technische Universität München, 80802 München, Germany

In the mammalian retina, besides the conventional rod–cone system, a melanopsin-associated photoreceptive system exists that conveys photic information for accessory visual functions such as pupillary light reflex and circadian photo-entrainment^{1–7}. On ablation of the melanopsin gene, retinal ganglion cells that normally express melanopsin are no longer intrinsically photosensitive⁸. Furthermore, pupil reflex⁸, light-induced phase delays of the circadian clock^{9,10} and period lengthening of the circadian rhythm in constant light^{9,10} are all partially impaired. Here, we investigated whether additional photoreceptive systems participate in these responses. Using mice lacking rods and cones, we measured the action spectrum for phase-shifting the circadian rhythm of locomotor behaviour. This spectrum matches that for the pupillary light reflex in mice of the same genotype¹¹, and that for the intrinsic photosensitivity of the melanopsin-expressing retinal ganglion cells⁷. We have also generated mice lacking melanopsin coupled with disabled rod and cone phototransduction mechanisms. These animals have an intact retina but fail to show any significant pupil reflex, to entrain to light/dark cycles, and to show any masking response to light. Thus, the

rod–cone and melanopsin systems together seem to provide all of the photic input for these accessory visual functions.

Rods and cones have long been thought to be the exclusive photoreceptors in the retina. This hypothesis is now known to be untrue. An opsin-like protein called melanopsin, originally identified in *Xenopus* skin melanophores¹, is present in a small subset of mammalian retinal ganglion cells (RGCs)^{1–6}, and these cells are intrinsically photosensitive^{6,7}. The axons of these RGCs project predominantly to the suprachiasmatic nucleus (SCN), the intergeniculate leaflet (IGL) and the olivary pretectal nucleus (OPN) of the brain⁶, which are key centres for circadian photo-entrainment and the pupillary light reflex. In melanopsin knockout mice (*Opn4*^{-/-}, formerly referred to as *mop*^{-/-}; see ref. 8), those RGCs that would normally express melanopsin lose their intrinsic photosensitivity⁸. *Opn4*^{-/-} mice also have an incomplete pupillary light reflex at high illuminations⁸. In independently produced melanopsin-knockout mice, others have found that the ability of light to phase-delay and lengthen the period of the circadian rhythm is also diminished^{9,10}. For the pupil reflex, this photic response can be quantitatively accounted for by a functional complementarity between the rod–cone system and the melanopsin system, without the need to invoke any additional light-detection system⁸. Nonetheless, the proposal has persisted that cryptochromes—flavoproteins reported to have a direct light-detecting role in *Drosophila*^{12,13}—may have the same function in mammals^{14–16} despite earlier evidence to the contrary¹⁷. To settle this question, we first examined the action spectrum for phase-shifting the circadian rhythm in mice lacking rod and cone photoreceptors (*rd/rd cl*)¹⁸. Next, we generated triple-knockout mice lacking all confirmed photodetection systems—*Opn4*^{-/-} *Gnat1*^{-/-} *Cnga3*^{-/-} (melanopsin (also known as opsin 4), guanine nucleotide-binding protein α -transducin 1 (also known as rod transducin α -subunit, or Tr α) and cyclic GMP-gated channel A-subunit 3, respectively)—and tested these animals for pupil reflex, circadian photo-entrainment and the masking response to light.

Irradiance–response relations for the light-induced phase shifting of the circadian rhythm of locomotor behaviour in *rd/rd cl* mice were measured at various wavelengths (Fig. 1a). The irradiance for half-maximal phase shift at each wavelength was then plotted to give the action spectrum (Fig. 1b). This spectrum is best fitted by the predicted absorption spectrum of a vitamin A₁-based photopigment with a wavelength of maximum absorbance (λ_{\max}) \approx 481 nm, similar to that for the pupil reflex in this genotype ($\lambda_{\max} \approx$ 479 nm)¹¹ and, more specifically, that for the intrinsically photosensitive, melanopsin-expressing RGCs in the rat ($\lambda_{\max} \approx$ 484 nm)⁷. Thus in the absence of rods and cones, circadian photo-entrainment is apparently determined by the melanopsin system. Previously, an action spectrum with a λ_{\max} of 480 nm has been reported for

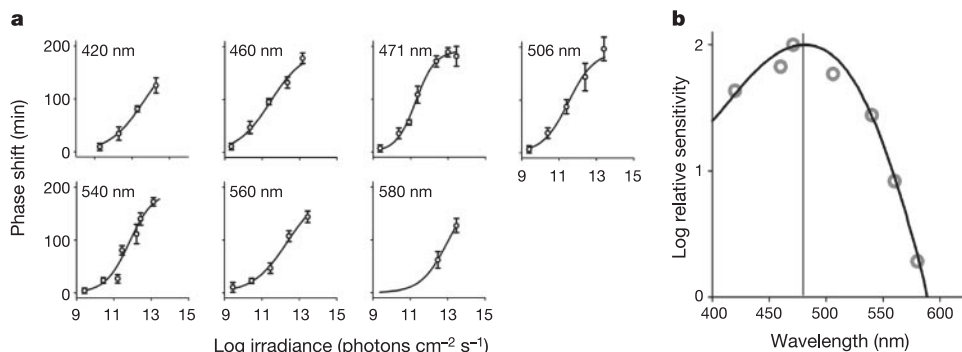


Figure 1 Irradiance–response relations (**a**) and action spectrum (**b**) for circadian phase shifting in *rd/rd cl* mice by monochromatic light between 420 nm and 580 nm, assayed by wheel-running ($n = 4–7$ animals per irradiance at each wavelength). The derived action

spectrum in **b** for circadian photo-entrainment is best fitted ($R^2 = 0.976$) by the absorption spectrum of a vitamin A₁-based photopigment with $\lambda_{\max} = 481$ nm (continuous curve).

circadian phase shifting by light in one strain of *rd* mice that has lost rods and perhaps most cones³¹. However, in part because the same experiments on a different strain of *rd* mice gave a λ_{\max} between 500 nm and 515 nm (ref. 32) and interpreted to reflect the action spectrum of mouse middle-wavelength-sensitive (M)-cones, the significance of the first study was never settled. With the *rd/rd cl* mouse line described here in which the loss of rods and cones is essentially complete, however, the signal from residual cones is no longer an issue.

To obtain more conclusive evidence that no other independent photoreceptive systems exist for the various accessory visual functions, we generated triple-knockout mice in which the rod–cone system and the melanopsin system were both silenced. Notably, the silencing of rod–cone functions in this case was achieved not by inducing degeneration of these cells (as occurs in *rd/rd cl* mice) but by combining targeted deletions of the genes for rod *Gnat1* (ref. 19) and cone *Cnga3* (refs 20, 21). *Gnat1* and *Cnga3* are critically involved in the G-protein-coupled cGMP signalling pathway that

mediates rod–cone phototransductions. Therefore, in triple-knock-out mice, the melanopsin system and the rod–cone system are both unable to signal light. We investigated whether these animals still had any residual response to light, as assayed by their pupil reflex and locomotor behaviour.

The *Opn4*^{-/-} *Gnat1*^{-/-} *Cnga3*^{-/-} mice were generated by first producing triple heterozygotes (*Opn4*^{+/-} *Gnat1*^{+/-} *Cnga3*^{+/-}) and then mating these to homozygosity. These mice had a normal-looking retina (Fig. 2a). Because *Opn4*^{-/-} was produced by replacing the melanopsin gene with the tau-LacZ construct^{6,8}, the RGCs that would normally express melanopsin could be visualized by 5-bromo-4-chloro-3-indolyl- β -D-galactoside (X-gal) labelling.

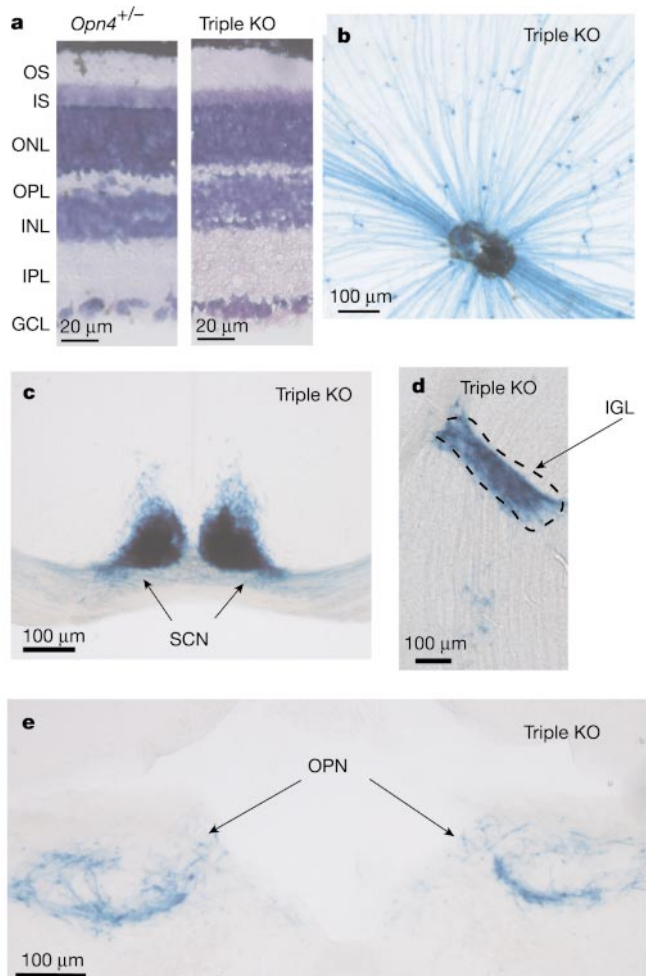


Figure 2 Normal retinal morphology and presence and central connectivity of melanopsin-expressing RGCs in triple-knockout (*Opn4*^{-/-} *Gnat1*^{-/-} *Cnga3*^{-/-}) mice. **a**, Retinal cross-sections from *Opn4*^{+/-} and triple-knockout (KO) mice. Giemsa stain shows the various layers. Both are similar in morphology and thickness to wild type. GCL, ganglion cell layer; INL, inner nuclear layer; IPL, inner plexiform layer; IS, inner segment layer; ONL, outer nuclear layer; OPL, outer plexiform layer; OS, outer segment layer. **b**, Flat-mount view of a triple-knockout retina stained with X-gal (blue). **c–e**, Coronal sections of triple-knockout mouse brain showing the normal innervations of the SCN, IGL and OPN by X-gal-labelled axons. Dorsal side is up in each case.

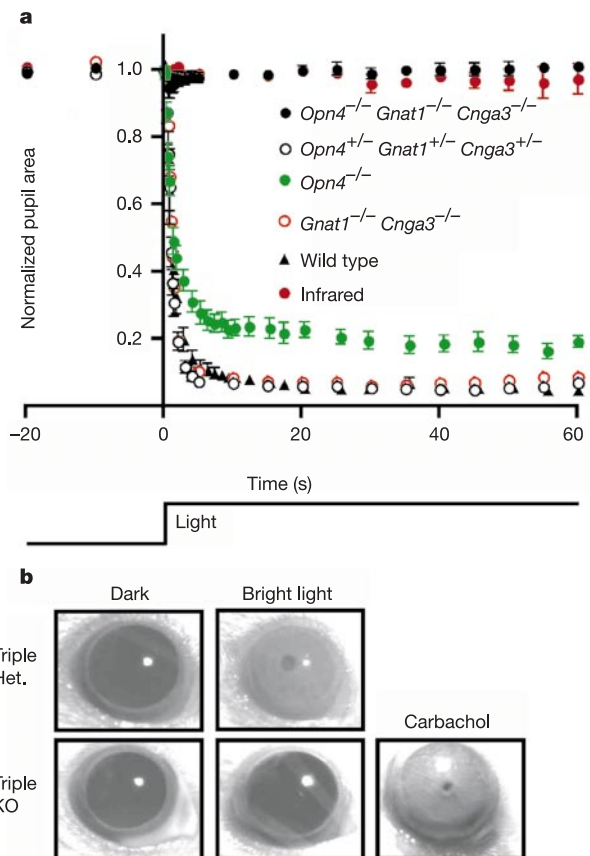


Figure 3 Disabling of rods, cones and melanopsin-positive RGCs essentially eliminates the pupillary light reflex. **a**, Pupil area (mean \pm s.e.m.) as a percentage of dark-adapted aperture area (recorded just before light exposure, time 0 on graph) for *Opn4*^{-/-} *Gnat1*^{-/-} *Cnga3*^{-/-} ($n = 6$), *Opn4*^{+/-} *Gnat1*^{+/-} *Cnga3*^{+/-} ($n = 4$), *Opn4*^{-/-} ($n = 8$; data reproduced from ref. 8) and *Gnat1*^{-/-} *Cnga3*^{-/-} ($n = 1$) mice over the course of 1 min when exposed to 480-nm light at 86–140 $\mu\text{W cm}^{-2}$. The wild-type data are from ref. 8. For comparison, the pupil size of triple-knockout mice exposed to an infrared light pulse ($n = 6$) is also shown. On close scrutiny, a small, transient pupil constriction was detected in two out of six triple-knockout mice exposed to the intense 480-nm stimulus. The averaged 480-nm data shown for the triple knockouts are from mice dark-adapted for 3 days before light exposure, but are representative of similar recordings from the same group after 1-h dark adaptation. Neither the amplitude nor the frequency of occurrence of the residual pupillary response in the triple-knockout animals were increased with bright white-light stimulus (30 mW cm^{-2}), or with monochromatic stimuli ranging from 360 to 660 nm (70 $\mu\text{W cm}^{-2}$ at 360 nm; 19 $\mu\text{W cm}^{-2}$ at 420 nm; 86 $\mu\text{W cm}^{-2}$ at 480 nm; 100 $\mu\text{W cm}^{-2}$ at 550 nm; 68 $\mu\text{W cm}^{-2}$ at 660 nm). Nor did these parameters show any significant change when tested repeatedly over a 24-h period. **b**, Application of 100-mM carbachol resulted in a complete pupil constriction in triple-knockout mice.

In the triple-knockout mice, these cells were still present (Fig. 2b) in numbers (about 600 per retina) comparable to wild type^{6,8}, and their axons still projected predominantly to the SCN, IGL and OPN of the brain (Fig. 2c–e). Thus, the absence of melanopsin and of functional rod–cone phototransductions does not affect the genesis, survival and central connectivity of the melanopsin-associated RGCs.

When tested for the pupillary light reflex with steady, intense exposure of light at 480 nm, the triple-heterozygous mice gave a response resembling wild type in amplitude and time course (Fig. 3a). The double-knockout mice (*Gnat1*^{-/-} *Cnga3*^{-/-}) showed the same response (Fig. 3a), similar to what we found previously¹¹ for *rd/rd cl* mice, which have complete degeneration of rods and cones. Triple knockouts, however, hardly gave any response to the 480-nm stimulus (Fig. 3a), nor to monochromatic light at other wavelengths (360–660 nm) or intense white light (data not shown). The same general results were obtained when these animals were tested at various times over a 24-h period. On close inspection, there was a very transient, barely detectable pupil response (with a mean of 5% reduction in pupil area at peak response) in two out of six tested triple-knockout mice under exposure to bright 480-nm light. However, even in animals with this residual response was detected, it was not consistently present on repeated stimulus trials with extensive dark adaptation (up to 3 days) in between (see Fig. 3 legend). The response was unlikely to be caused by heat associated with the illumination, because it largely disappeared after replacement of the 480-nm interference filter with a band-pass filter transmitting only infrared light (≥ 850 nm) (Fig. 3a). A possible source of the signal is the early receptor potential of rods and cones, which consists of a very small, transient membrane hyperpolarization caused by charge movements associated with conformational changes of the visual pigments after photo-isomerization^{22,23}. This hyperpolarization should persist regardless of whether the transduction steps downstream of the pigment are disabled or not. Another possibility is a very small, transient hyperpolarization generated by intense light in rods and cones via a pathway apparently independent of transducin²⁴. In any

case, the smallness of the residual pupil response, its transient nature even in steady, intense light, and the inconsistency of its occurrence all suggest that it is unlikely to be of physiological significance. Finally, the failure of the *Opn4*^{-/-} *Gnat1*^{-/-} *Cnga3*^{-/-} pupil to constrict was not due to a defect in the constriction mechanism because carbachol, a parasympathetic agonist, was able to activate maximum pupil constriction when applied to the cornea (Fig. 3b).

To assess photo-entrainment, *Opn4*^{+/-} *Gnat1*^{+/-} *Cnga3*^{+/-} and *Opn4*^{-/-} *Gnat1*^{-/-} *Cnga3*^{-/-} animals separate from those used in the pupil-reflex studies were kept in an 16/8-h light/dark cycle (800 lx white light in the light period), and their locomotor activity was monitored (see Methods). The triple-heterozygous mice showed normal photo-entrainment, whereas the triple-knockout mice did not show any entrainment (Fig. 4; see also Supplementary Information). Actograms indicated that the triple-heterozygous mice had an average period length of 24.0 ± 0 h (mean \pm s.e.m., $n = 6$; individually all 24.0 h), as expected from stable photo-entrainment. In contrast, the triple homozygous mice had a period length of 23.3 ± 0.2 h ($n = 5$; individually 23.8, 23.3, 23.2, 22.5 and 23.5 h), similar to the 23.6 h reported for the same strain (B6/129) of wild-type mice in constant darkness²⁵, indicating that these animals free-ran even under light/dark conditions. Of note, at the light intensity used in these experiments, the pupils of wild-type or triple-heterozygous mice would have constricted considerably (see Fig. 3a), whereas those of the triple-knockout mice would have stayed unchanged. Thus, the equivalent light intensity at which the triple-knockout mice failed to show photo-entrainment was actually much higher than that capable of entraining wild-type or triple-heterozygous mice.

We have also examined another accessory visual function, namely the masking of locomotion of nocturnal rodents by light, which involves a fast and direct effect of light independent of the circadian pacemaker^{26–28}. To examine masking by light, the mice tested for photo-entrainment were subsequently placed on a 3.5/3.5-h light/dark cycle (800 lx white light as before, although the equivalent intensity for the triple-knockout mice would again be considerably

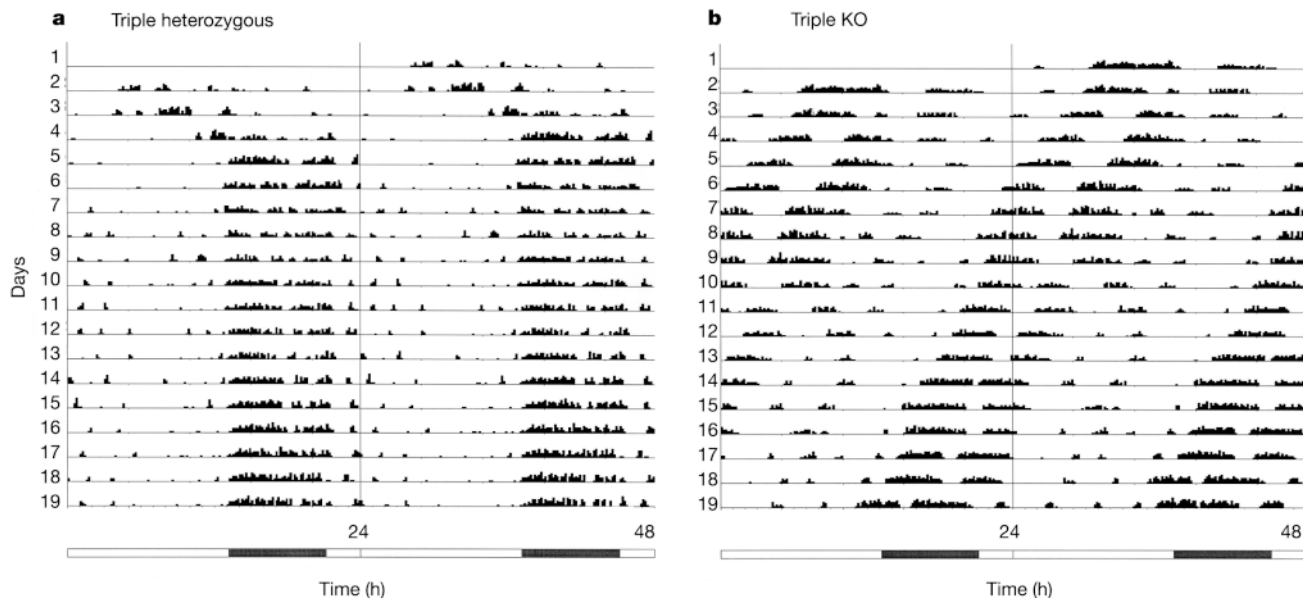


Figure 4 Actograms of wheel running for mice under a 16/8-h light/dark cycle, double-plotted on a 24-h timescale. The illumination was approximately 800 lx white light. The numbered lines represent successive days. Activity levels (in total number of revolutions in 10-min bins) are given in 15 quantiles, with the first being 1–55 revolutions, the second 56–110, and so on. The bar below the actograms indicates light (white) and dark (black)

periods. **a**, Triple heterozygote (*Opn4*^{+/-} *Gnat1*^{+/-} *Cnga3*^{+/-}). The locomotor activity had a cycle very close to 24 h and was phase-locked to darkness, showing photo-entrainment. **b**, Triple-knockout (*Opn4*^{-/-} *Gnat1*^{-/-} *Cnga3*^{-/-}). The animal free-ran with a period of less than 24 h, showing lack of photo-entrainment.

higher than for the triple-heterozygous mice when the lack of pupil reflex in the triple-knockout animals is taken into account). This ultradian cycle is useful for assessing masking because it is difficult to entrain circadian rhythms to cycles with periods of 7 h or multiples thereof. In this way, it was ensured that masking could be measured at different phases of the endogenous clock²⁹. When kept in this cycle, the triple-heterozygous mice showed two effects. Four of the six tested animals were negatively masked (that is, their locomotor activity was diminished) by light (Fig. 5a). The average percentage of activity in the dark period for these 'light avoiders' was $87.1 \pm 8.8\%$ (mean \pm s.e.m.; individually 99.5%, 66.3%, 85.0% and 97.7%), similar to what was seen with B6/129 wild-type mice ($n = 12$; N.M. and S.H., unpublished data). The remaining two animals, paradoxically, developed more wheel-running activity in the light period (Fig. 5b), possibly due to the presence of the 129-strain background associated with the triple-heterozygous genotype (this activity reversal has previously been observed in other mouse lines with the 129-strain background; R.J.L., unpublished data). Although the reason for this reversal of activity with respect to the light/dark cycle is unclear, undoubtedly light still had an effect (in this case, positive masking). The percentage of activity in the dark period for these two 'light preferers' was 32.7% (Fig. 5b) and 26.0%, respectively. The triple-knockout mice, on the other hand, were hardly affected by this ultradian light/dark cycle (Fig. 5c, d). The average percentage of activity in the dark period was $43.2 \pm 3.4\%$ (mean \pm s.e.m., $n = 4$; individually 44.7%, 50.5%, 40.8% and 36.6%), much closer to that expected from randomness (50%).

Given the fact that RGCs normally expressing melanopsin still project to the appropriate brain targets in triple-knockout mice, the conclusion from our experiments is that the rod-cone system and the melanopsin system are the exclusive light-detecting systems in the eye for producing the normal pupillary light reflex, photo-entrainment and masking response to light. These experiments go beyond our previous conclusion that the rod-cone and melanopsin systems are fully complementary to each other in the pupil reflex⁸, by demonstrating an essentially complete loss of this and other functions when the two systems are absent or disabled. It was recently reported¹⁶ that the pupil reflex of mice lacking rods as well as Cry1 and Cry2 (*rd/rd Cry1^{-/-} Cry2^{-/-}*) is 100-fold less photosensitive than normal (and 10-fold less sensitive than mice only lacking rods; *rd/rd*), proposed to support the idea that the cryptochromes may participate as a photodetective system. Nonetheless, other interpretations of these earlier data are possible. Furthermore, the pupil reflex of mice only lacking Cry1 and Cry2 is normal (as is their masking response to light³⁰). A potential complicating factor in interpreting the results from mice lacking Cry1 and Cry2 is that these animals are reported to show frequent ocular inflammation¹⁵, which may cause subtle changes in retinal function. In any case, we know from immunocytochemistry of our *Opn4^{-/-} Gnat1^{-/-} Cnga3^{-/-}* mice that at least Cry2 is still widely expressed in the inner retina (including the RGCs expressing melanopsin), comparable to wild type (data not shown)—the antibodies for Cry1 did not give informative labelling; see Methods. At the same time, real-time polymerase chain reaction with reverse transcription (RT-PCR) indicated that the message levels for Cry1

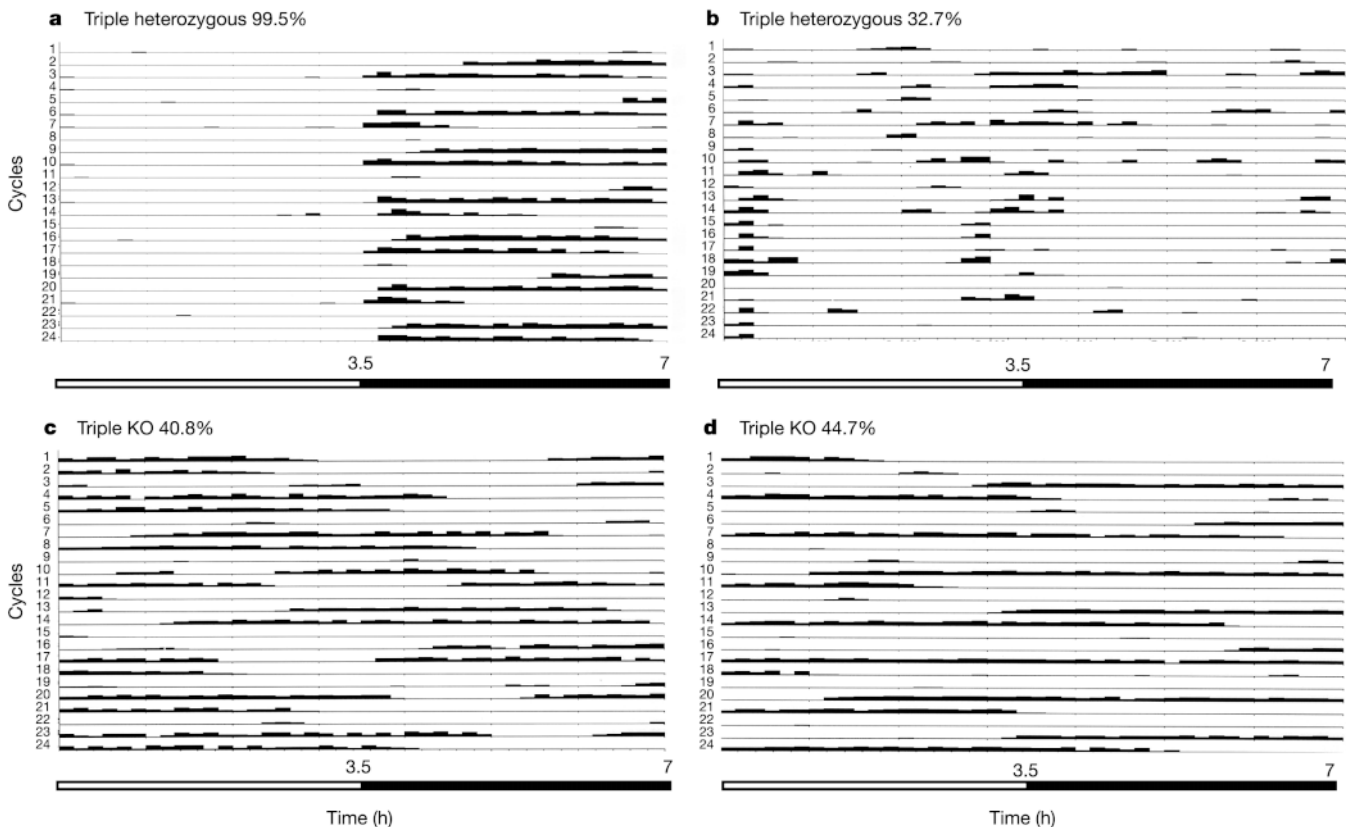


Figure 5 Actograms of wheel running plotted on a 7-h timescale. The mice were subjected to an ultradian 3.5/3.5-h light/dark cycle (see text). Illumination was approximately 800 lx white light. The numbered lines represent successive 7-h cycles. The activity quantiles and time bins are the same as in Fig. 4. **a, b**, Two triple-heterozygous mice (*Opn4^{+/-} Gnat1^{+/-} Cnga3^{+/-}*) showing a negative and positive

masking effect, respectively. The percentage of total revolutions in darkness was 99.5% and 32.7%, respectively. **b**, Two triple-knockout mice (*Opn4^{-/-} Gnat1^{-/-} Cnga3^{-/-}*). The percentage of total revolutions in darkness was 40.8% and 44.7%, respectively, not far from the 50% expected from randomness; that is, no masking effect of light.

and *Cry2* in *Opn4^{-/-} Gnat1^{-/-} Cnga3^{-/-}* eyes are comparable to those in wild-type mice (Supplementary Information). Thus, the disappearance of the accessory visual functions in the triple-knockout mice cannot be attributed to secondary loss of cryptochromes. Even if mammalian cryptochromes should turn out to function as direct light detectors, either they obligatorily depend on the presence of melanopsin for their light-detecting function or they do not signal light at least for the diverse photic responses studied here. □

Methods

Animals

The *rd/rd cl* mice were bred at Imperial College London, and the circadian phase-shifting experiments were carried out there. The triple-knockout and the corresponding triple-heterozygous mice were bred at Johns Hopkins. The pupil reflex experiments were done at Hopkins, whereas the wheel-running experiments were done at the University of Toronto. At the time of experimentation, the Hopkins animals were 1–4 months old for the pupil reflex measurements and 1–9 months old (1–9 months for triple-heterozygous mice, 1–2 months for triple-knockout mice; all were males except for one female triple knockout, which was used for photo-entrainment but not for masking experiments) for the wheel-running measurements. For morphological, X-gal labelling, immunocytochemical and RT-PCR experiments, the animals were 2–3 months old.

Giemsa staining of retinal cross-sections

An animal anaesthetized by intraperitoneal injection of avertin (0.2 ml g⁻¹) was circulationally perfused with 25 ml cold 4% paraformaldehyde in PBS for 15 min. The eyes were isolated, corneas removed, and fixed for an additional 3 h in cold 4% paraformaldehyde in PBS. The eyes were cryo-protected overnight in 30% sucrose in PBS at 4 °C, then sectioned at 10 µm thickness on a cryostat. The sections were allowed to dry and stained with the nucleus-labelling Giemsa solution (Sigma).

Assays for *Cry1* and *Cry2* in triple-knockout eyes

We used two assays. The first was immunocytochemistry⁶, with antibodies PA1-527 (Affinity Bioreagents) and CRY11-A (Alpha Diagnostic International) against *Cry1*, and CRY21-A (Alpha Diagnostic International) against *Cry2*. The two antibodies against *Cry1* did not give specific labelling in the retina, but *Cry2* gave labelling specific enough for comparison with wild-type retina. The second assay was with RT-PCR using *Cry1*- and *Cry2*-specific primers. The samples were whole eyes without the lens, and RNA was extracted using the trizol method (Sigma). The controls were RNA samples without reverse transcriptase. Real-time RT-PCR was carried out with SYBR green detection on an ABI Prism 7700 machine (Applied Biosystems). The identity of the product was checked by melting-curve analysis, size confirmation on an agarose gel and sequencing of the products.

X-gal staining

For X-gal labelling of the brain sections or flat-mount retina of the triple-knockout mice, an animal was anaesthetized and circulationally perfused with fixative as above, and the brain/eyes were isolated. An eye-cup was prepared by removing the anterior half of the eye, while the brain was frozen on dry ice and sectioned at 50-µm thickness with a sliding microtome (Leica SM2000R). Brain sections were mounted on microscope slides (Fisherbrand, superfrost-plus) and allowed to dry overnight. To stain for β-galactosidase activity, both preparations were washed twice in buffer B (100 mM phosphate buffer, pH 7.4, 2 mM MgCl₂, 0.01% Na-desoxycholate and 0.02% (octylphenoxy) polyethoxyethanol (IGEPAL)), and then incubated in the staining solution (buffer B plus 5 mM K-ferricyanide, 5 mM K-ferrocyanide and 1 mg ml⁻¹ X-gal) for 6–10 h at room temperature in darkness. Afterwards, the retina was isolated from the eye-cup and flat mounted. Both brain sections and the retina were mounted in glycerol. Images were obtained using a Zeiss Axiophot microscope and AxioCam HRC digital camera.

Phase shifting of locomotion in *rd/rd cl* mice

Singly housed male C3H/He *rd/rd cl* mice aged between 80 and 250 days were maintained in constant darkness. A single 15-min monochromatic light pulse (half bandwidth = 10 nm) of defined irradiance was applied after 7 days at circadian time 16 (4 h after activity onset) at 420, 460, 471, 506, 540, 560 and 580 nm, respectively. To correct for lens transmission at different wavelengths, lenses were extracted from *rd/rd cl* mice (*n* = 4) and wavelength-scanned in air using an integrating sphere (see Supplementary Information). The irradiances indicated have been corrected for lens transmission. The magnitude of phase shift in free-running locomotor activity rhythm by light at each wavelength was plotted against irradiance and fitted to a sigmoidal function. The irradiances that produced half-maximum phase shifts were plotted against wavelength to produce the action spectrum. This spectrum was fitted with the absorption spectrum of a vitamin A₁-based pigment with a best-fit λ_{max} determined by least squares.

Pupillometry

Consensual pupillary constriction was measured in response to an adirectional light stimulus. Light was provided by a PTI xenon arc-lamp, filtered to remove wavelengths <299 nm and most infrared, and transmitted by means of a liquid light guide to a diffusing sphere. This sphere was constructed from a ping-pong ball and designed to render the light stimulus nearly adirectional at the location of the mouse cornea. An adult

mouse, dark-adapted for 1 h and unanaesthetized, was positioned and oriented with the help of an infrared image-converter such that one eye was situated at the exit of the reflective sphere and the other eye was in focus, and oriented as perpendicular as possible, to a charge-coupled device (CCD) camera fitted with a ×10 macro lens. Illumination of the videoed eye was with infrared LEDs (>850 nm) throughout the experiment. Pupil measurements from the video images of the eye were made using TINA 3.1 image-analysis software and a Matrox meteor-II frame-grabber card (Matrox Imaging). The intensity and wavelength of the light stimulus were controlled with calibrated neutral-density and interference (10-nm bandwidth) filters. Irradiance measurements (W cm⁻²) were made with a radiometer (Macam Photometrics). Unless indicated otherwise, all experiments reported here were conducted during the light period of a 14/10-h light/dark cycle (between 9 and 3 h before lights off)⁸.

Carbachol application

Carbachol (carbamylcholine chloride) was obtained from Sigma. Solution (100 mM) was prepared in ×1 PBS, pH 7.4, and filtered through a 0.22-µm filter. Samples were topically applied to the cornea of the mouse eye with a microtip transfer pipette. The pupil size in darkness was assessed immediately before and at 5 min after carbachol application. We found that a carbachol concentration of 100 mM was able to fully constrict the eyes of both triple-heterozygous and triple-knockout mice, and therefore we did not use higher concentrations (see ref. 8).

Photo-entrainment and masking experiments

The mice were placed individually in cages (44 × 23 × 20 cm) equipped with running wheels (17.5 cm in diameter). Room temperature was 19.5–23.5 °C. Revolutions were recorded with Dataquest III hardware and software in 10-min bins. The light/dark cycle was 16/8-h light/dark or 3.5/3.5-h light/dark, with approximately 800 lx in the light period (Hagner EX2 luxmeter) illuminated by Sylvania Octron 32 W 4100K fluorescent tubes. For photo-entrainment, the animals were studied for 19 days on the 16/8-h light/dark cycle, with data from the last 10 days used for period analysis based on the algorithm of Clocklab (Actimetrics) for the Bushell and Sokolov χ² periodogram. For masking, the animals were kept on the ultradian 3.5/3.5-h light/dark cycle for 11 days. Data from the last 7 days, which covered light and dark periods spanning the entire circadian cycle, were used for calculating the percentages of wheel-running activity in darkness.

Received 21 April; accepted 2 June 2003; doi:10.1038/nature01761.

Published online 15 June 2003.

1. Provencio, I., Jiang, G., DeGrip, W. J., Hayes, W. P. & Rollag, M. D. Melanopsin: an opsin in melanophores, brain, and eye. *Proc. Natl Acad. Sci. USA* **95**, 340–345 (1998).
2. Provencio, I. *et al.* A novel human opsin in the inner retina. *J. Neurosci.* **20**, 600–605 (2000).
3. Gooley, J. J., Lu, J., Chou, T. C., Scammell, T. E. & Saper, C. B. Melanopsin in cells of origin of the retinohypothalamic tract. *Nature Neurosci.* **4**, 1165 (2001).
4. Hannibal, J., Hindersson, P., Knudsen, S. M., Georg, B. & Fahrenkrug, J. The photopigment melanopsin is exclusively present in pituitary adenylate cyclase-activating polypeptide-containing retinal ganglion cells of the retinohypothalamic tract. *J. Neurosci.* **22**, RC191 (2002).
5. Provencio, I., Rollag, M. D. & Castrucci, A. M. Photoreceptive net in the mammalian retina. *Nature* **415**, 493 (2002).
6. Hattar, S., Liao, H.-W., Takao, M., Berson, D. M. & Yau, K.-W. Melanopsin-containing retinal ganglion cells: architecture, projections, and intrinsic photosensitivity. *Science* **295**, 1065–1070 (2002).
7. Berson, D. M., Dunn, F. A. & Takao, M. Phototransduction by retinal ganglion cells that set the circadian clock. *Science* **295**, 1070–1073 (2002).
8. Lucas, R. J. *et al.* Diminished pupillary light reflex at high irradiances in melanopsin-knockout mice. *Science* **299**, 245–247 (2003).
9. Panda, S. *et al.* Melanopsin (*Opn4*) requirement for normal light-induced circadian phase shifting. *Science* **298**, 2213–2216 (2002).
10. Ruby, N. F. *et al.* Role of melanopsin in circadian responses to light. *Science* **298**, 2211–2213 (2002).
11. Lucas, R. J., Douglas, R. H. & Foster, R. G. Characterization of an ocular photopigment capable of driving pupillary constriction in mice. *Nature Neurosci.* **4**, 621–626 (2001).
12. Emery, P., So, W. V., Kaneko, M., Hall, J. C. & Roshbash, M. *CRY*, a *Drosophila* clock and light-regulated cryptochrome, is a major contributor to circadian rhythm resetting and photosensitivity. *Cell* **95**, 669–679 (1998).
13. Ceriani, M. F. *et al.* Light-dependent sequestration of TIMELESS by CRYPTOCHROME. *Science* **285**, 553–556 (1999).
14. Selby, C. P., Thompson, C., Schmitz, T. M., van Gelder, R. N. & Sancar, A. Functional redundancy of cryptochromes and classical photoreceptors for nonvisual ocular photoreception in mice. *Proc. Natl Acad. Sci. USA* **97**, 14697–14702 (2000).
15. van Gelder, R. N. Non-visual ocular photoreception. *Ophthalmic Genet.* **22**, 195–205 (2001).
16. van Gelder, R. N., Wee, R., Lee, J. A. & Tu, D. C. Reduced pupillary light responses in mice lacking cryptochromes. *Science* **299**, 222 (2003).
17. Griffin, E. A. Jr, Staknis, D. & Weitz, C. J. Light-independent role of CRY1 and CRY2 in the mammalian circadian clock. *Science* **286**, 768–771 (1999).
18. Lucas, R. J., Freedman, M. S., Munoz, M., Garcia-Fernandez, J. M. & Foster, R. Regulation of the mammalian pineal by non-rod, non-cone, ocular photoreceptors. *Science* **284**, 505–507 (1999).
19. Calvert, P. D. *et al.* Phototransduction in transgenic mice after targeted deletion of the rod transducin α-subunit. *Proc. Natl Acad. Sci. USA* **97**, 13913–13918 (2000).
20. Biel, M. *et al.* Selective loss of cone function in mice lacking the cyclic nucleotide-gated channel CNG3. *Proc. Natl Acad. Sci. USA* **96**, 7553–7557 (1999).
21. Bradley, J., Frings, S., Yau, K.-W. & Reed, R. Nomenclature for ion channel subunits. *Science* **294**, 2095–2096 (2001).
22. Cone, R. A. Early receptor potential: photoreversible charge displacement in rhodopsin. *Science* **155**, 1128–1131 (1967).
23. Murakami, M. & Pak, W. L. Intracellularly recorded early receptor potential of the vertebrate photoreceptors. *Vision Res.* **10**, 965–975 (1970).

24. Brockerhoff, S. E. *et al.* Light stimulates a transducin-independent increase of cytoplasmic Ca²⁺ and suppression of current in cones from the zebrafish mutant *nof*. *J. Neurosci.* **23**, 470–480 (2003).
 25. Wee, R., Castrucci, A. M., Provencio, I., Gan, L. & van Gelder, R. N. Loss of photic entrainment and altered free-running circadian rhythms in *math5*^{-/-} mice. *J. Neurosci.* **22**, 10427–10433 (2002).
 26. Aschoff, J. in *Trends in Chronobiology. Advances in the Biosciences* Vol. 73 (eds Hekkens, W. T. J. M., Kerkhof, G. A. & Rietveld, W. J.) 149–161 (Pergamon, Oxford, 1988).
 27. Mrosovsky, N. Masking: history, definitions, and measurement. *Chronobiol. Int.* **16**, 415–429 (1999).
 28. Mrosovsky, N., Lucas, R. J. & Foster, R. G. Persistence of masking responses to light in mice lacking rods and cones. *J. Biol. Rhythms* **16**, 585–587 (2001).
 29. Redlin, U. & Mrosovsky, N. Masking of locomotor activity in hamsters. *J. Comp. Physiol. A* **184**, 429–437 (1999).
 30. Mrosovsky, N. Further characterization of the phenotype of *mCry1/mCry2*-deficient mice. *Chronobiol. Int.* **18**, 613–625 (2001).
 31. Yoshimura, T. & Ebihara, S. Spectral sensitivity of photoreceptors mediating phase-shifts of circadian rhythms in retinally degenerate CBA/J (*rd/rd*) and normal CBA/N (+/+) mice. *J. Comp. Physiol. A* **178**, 797–802 (1996).
 32. Provencio, I. & Foster, R. G. Circadian rhythms in mice can be regulated by photoreceptors with cone-like characteristics. *Brain Res.* **694**, 183–190 (1995).

Supplementary Information accompanies the paper on www.nature.com/nature.

Acknowledgements We thank H.-W. Liao and J. Lai for help in performing the immunocytochemical experiments with antibodies against cryptochromes; J. Butler for help with real-time RT-PCR; Y. Liang for help in genotyping the animals; P. Salmon for help in the wheel-running experiments; and D. M. Berson, H. R. Matthews, G. L. Fain and members of the Yau laboratory for scientific discussions. This work was supported by the US National Eye Institute (K.-W.Y.), the UK Biotechnology and Biological Sciences Research Council and the Wellcome Trust (R.J.L. and R.G.F.), and the Canadian Institutes of Health Research (N.M.).

Competing interests statement The authors declare that they have no competing financial interests.

Correspondence and requests for materials should be addressed to K.-W.Y. (kwyau@mail.jhmi.edu).

A TRPV family ion channel required for hearing in *Drosophila*

Janghwan Kim^{†*}, Yun Doo Chung^{‡§}, Dae-young Park^{*}, Sookyung Choi^{*}, Dong Wook Shin^{*}, Heun Soh^{||}, Hye Won Lee^{*}, Wonseok Son^{*}, Jeongbin Yim[¶], Chul-Seung Park^{||}, Maurice J. Kernan^{‡§} & Changsoo Kim^{*}

* Department of Genetics, Hanwha Chemical Co. R&D Center, Sinsung-Dong, Yusung-Gu, Daejeon 305-345, Korea

† Department of Microbiology, Chungnam National University, Daejeon 305-764, Korea

‡ Department of Neurobiology & Behavior, and § Center for Developmental Genetics, State University of New York at Stony Brook, New York 11794, USA

|| Department of Life Science, K-JIST, Gwangju 500-712, Korea

¶ National Creative Research Institute for Genetic Reprogramming, Seoul National University, Seoul 151-742, Korea

The many types of insect ear share a common sensory element, the chordotonal organ, in which sound-induced antennal or tympanal vibrations are transmitted to ciliated sensory neurons and transduced to receptor potentials^{1,2}. However, the molecular identity of the transducing ion channels in chordotonal neurons, or in any auditory system, is still unknown^{3,4}. *Drosophila* that are mutant for NOMPC, a transient receptor potential (TRP) superfamily ion channel, lack receptor potentials and currents in tactile bristles^{5,6} but retain most of the antennal sound-evoked response⁷, suggesting that a different channel is the primary transducer in chordotonal organs. Here we describe the *Drosophila* Nanchung (Nan) protein, an ion channel subunit similar to vanilloid-receptor-related (TRPV) channels of the TRP superfamily. Nan mediates hypo-osmotically activated calcium influx and cation currents in cultured cells. It is expressed *in vivo* exclusively in chordotonal neurons and is localized to their

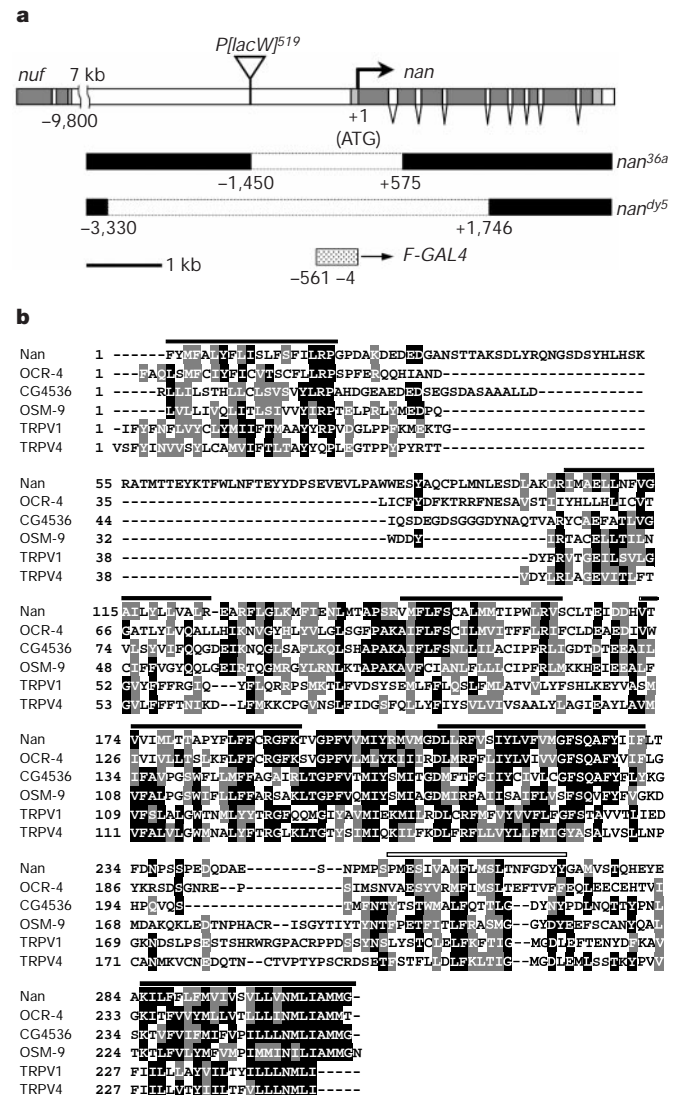


Figure 1 Molecular analysis of *nan*. **a**, Genomic organization. A transcription start site at -91 with respect to the translation start (+1) is indicated (angled arrow). A P transposon (*P[lacW]*⁵¹⁹) inserted 1.4-kb upstream of the transcription start site was imprecisely excised to give the deletions *nan*^{36a} and *nan*^{dy5}, deleting 150 and 478 codons, respectively. The *F-GAL4* construct contains a 557-bp fragment (dotted box). **b**, Alignment of the transmembrane region from TRPV proteins, including *Drosophila* Nan and CG4536, *C. elegans* OCR-4 and OSM-9, and human TRPV1 and TRPV4. Transmembrane domains (closed bars) and a putative pore region (open bar) were predicted by TMHMM2.0 (ref. 25). Black shading, identical amino acids; grey shading, similar amino acids; as used by Boxshade program (www.ch.embnet.org). **c**, Topology model for Nan protein, based on SMART²⁶ and TMHMM2.0 predictions. The putative pore region is denoted by a closed circle. **d**, Phylogenetic tree of the TRPV ion channel subfamily, based on a CLUSTALW alignment.